Performance Assessment of a Multi-Rotor Floating Tidal Energy System

Nicholas Kaufmann, Ralf Starzmann and Nabil Al-Kahli

Abstract—**Performance assessments of full-scale tidal turbines successfully have been carried out for multiple machines deployed globally and reported in literature. While their general performance has been demonstrated, in the case of multi-rotor systems, like Sustainable Marine's floating tidal energy platforms, the potential interactions between the turbines, positive or negative, remain a key research question. In 2022 Sustainable Marine connected its latest development, the pre-commercial PLAT-I 6.40 platform, to the Canadian grid followed by a comprehensive commissioning and performance trials. PLAT-I 6.40 carries six 4m diameter SCHOTTEL Instream Turbines, each rated at 70 kW. This work presents a test campaign dedicated to the assessment of differences in the performance between the individual turbines. For this particular study, a flow speed sensor was sequentially positioned upstream of different turbines while a second flow measurement device was stationary as reference. For all test configurations the power curves of turbines and platform have been determined following the guidance of the IEC TS 62600-200. This paper presents the experimentally obtained power curves for each test configuration and compares it against the reference values. The results show that there are steady differences in the flow field resulting in varying power outputs across the different rotors. However, a comparison of the individual rotor power curves with the design predictions shows good agreement.**

Keywords—**Floating Tidal Platform, Full-Scale Tests, Field Tests, Power Curve Assessment, Multi-Rotor System**

I. Introduction

A broad variety of different full-scale devices to harness the energy of tidal currents has been successfully installed and operated in real sea conditions in recent years as summarized in [1]. These projects increase the operational experience, proving improved designs and ultimately path the way for cost-reduction, increased reliability and commercial usage. To these demonstration projects the performance assessment is a key measure, hence, a number of studies have been carried out and also reported in literature (e.g. [2]). The rotor number and diameter of the demonstrated tidal energy converters differs from single rotor devices in the MW class to scalable arrays of comparably small turbines. The basic idea behind multiple rotors carried by a single support structure, so called multi-rotor systems (MRS), is the opportunity for "scaling by quantity" rather than increasing the size of the rotor. The concept promises to improve the power to weight ratio and the robustness of the turbines, smaller tools and vessels are required for offshore maintenance operations and the smaller components de-risk the development (see e.g. [3] and [4]). Nonetheless, MRS require more complex support structures as compared to singe rotor devices [3]. The interaction between the rotors of MRS have been investigated in the wind (see e.g. [3] or [5]) and tidal sector (e.g. [6] and [7]), however, potential, positive or negative, remains a key research question, in particular in real sea conditions.

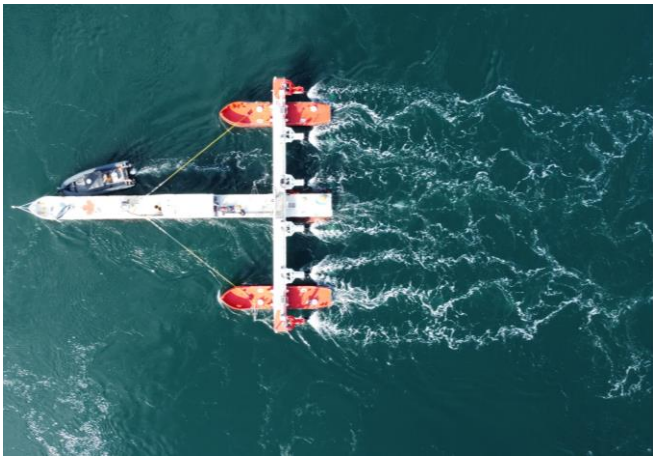

Fig. 1: Sustainable Marine's floating tidal energy platform PLAT-6.4 deployed in the Grand Passage, Nova Scotia, Canada

This work has been supported by Natural Resources Canada within Energy Innovation Program.

Nicholas Kaufmann is with SCHOTTEL HYDRO GmbH, Mainzer Str. 99, 56322 Spay, Germany (e-mail: nkaufmann@schottel.de)

Ralf Starzmann is with SCHOTTEL HYDRO GmbH, Mainzer Str. 99, 56322 Spay, Germany (e-mail: rstarzmann@schottel.de)

Nabil Al-Kahli (e-mail: nabil.alkahli@gmail.com)

Digital Object Identifier: https://doi.org/10.36688/ewtec-2023-365

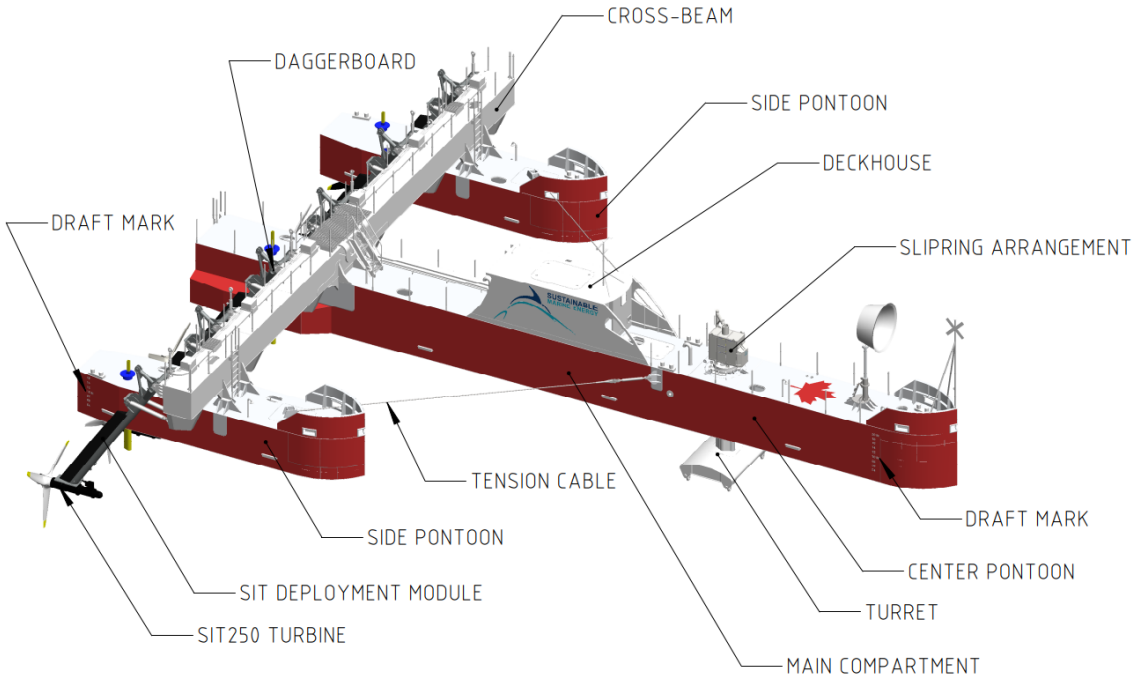

Fig. 2: Isometric model of PLAT-I 6.40 highlighting the key components.

Sustainable Marine has developed and built the pre-commercial MRS platform PLAT-I 6.40, shown in Fig. 1. PLAT-I 6.40 has been connected to the Canadian grid in May 2022. Between May and end of September 2022 the system has undergone comprehensive commissioning and performance trials. PLAT-I 6.40, carries six 4m diameter SCHOTTEL Instream Turbines (SIT), each rated at 70 kW. Previous studies, presented in [2], at the predecessor platform, Sustainable Marine's prototype system PLAT-I 4.63, have indicated that variations in the incoming flow field are likely to cause deviations in the performance of the platform's rotors.

The results presented in this paper are derived from a specific test campaign that has been conducted in the summer of 2022. The objectives of the tests were to investigate potential performance variations of the individual turbines and identify differences in the flow fields approaching them. To evaluate the variances in the flow field across all rotors, a flow speed sensor was sequentially positioned upstream of each turbine while a second flow measurement device was stationary as reference. For all test configurations the power curves have been determined following the guidance of the IEC TS 62600-200 [7]. Furthermore, the flow speeds measured at the different positions across the platform were compared against the reference measurements.

II. PLAT-I 6.40

A. *Platform*

PLAT-I 6.40 (Fig. 2) is Sustainable Marine (SME)'s second generation floating tidal energy platform. The three hulled platform is designed to host six of SCHOTEL HYDRO's Instream Turbines (SIT). The grid ready net capacity of PLAT-I is 420kW, with an overall length of 33.5m, overall breadth of 29m and design displacement of 140tons. Thanks to its shape and low draft, the platform offers an excellent stability and is operable in a wide range of weather and bathymetry conditions. The centre hull is sized to accept the electrical systems equipment and to provide most of the platform's buoyancy. The outer hulls are kept small to provide vessel stability whilst minimizing the bending moments imposed on the cross-deck structure. The cross-deck supports the turbines, which can be raised above water for tow and inspection, shown in Fig. 3. Tension cables are added from the side hulls to the main hull to further reduce the loads at the connection between the cross-deck and the main hull.

B. *SIT Deployment Modules*

To position the turbines in the flow, six SIT Deployment Modules (SDMs) are installed on the cross-deck of the platform. Fairings on the underwater portion

Fig. 3: SDM in raised position: turbines in parked position enabling easy access for inspection and maintenance.

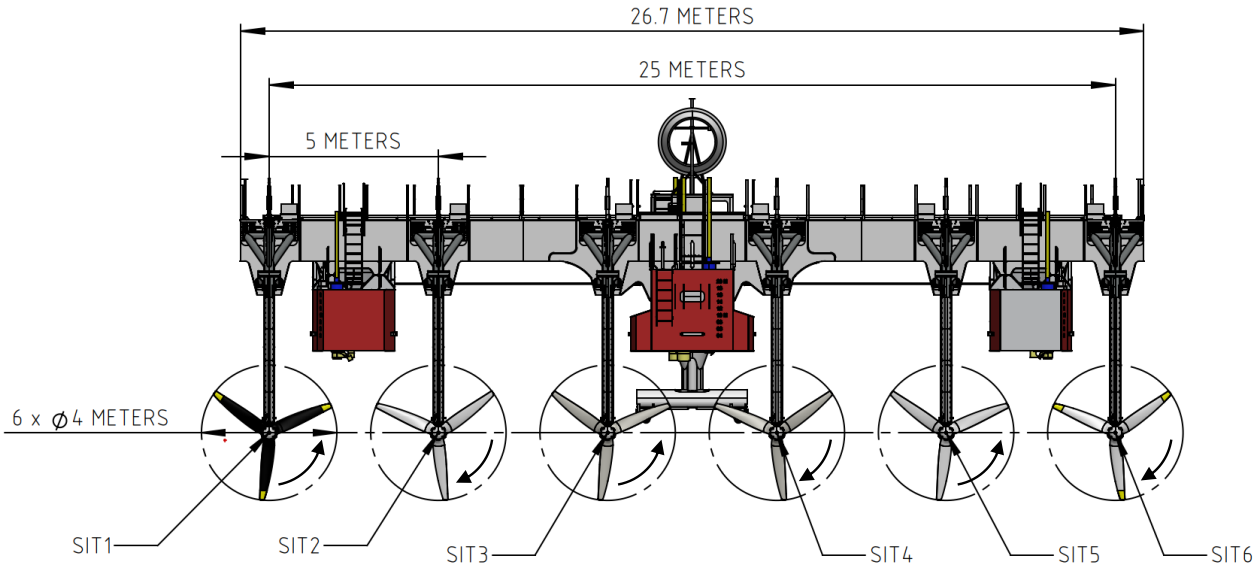

Fig. 4: Turbine spacing and rotational orientation on PLAT-I 6.40 looking into the flow.

help to minimize the drag and wake effects. Furthermore, an enclosed void space provides additional buoyancy. The fairings incorporate a channel for electrical and instrumentation cables. The SDMs are used to stop the turbines by lifting them above the water surface through hydraulic cylinders. The hydraulics provide an additional passive overload protection by allowing the SDMs to swing out of the flow in case of extreme load events. In the raised position, the drivetrains and blades are accessible from small work boats for inspection and maintenance. This grants an excellent accessibility to the key equipment at large weather and tidal windows without the necessity of rare and expensive special purpose vessels.

C. SCHOTTEL Instream Turbines

A total of six SITs are mounted in a downstream arrangement on PLAT-I 6.40 with a hub depth of 3m, three of them spinning clockwise, three of them spinning counter-clockwise. The horizontal distance between the rotational axes is 5 m, resulting in a tip clearance between the turbines of 0.25 diameters (1 m). An overview of the turbine arrangement on PLAT-I 6.40 is given in Fig. 4.

The SCHOTTEL Instream Turbine 250 (SIT 250) is a horizontal axis free flow, variable-speed-controlled turbine. The SIT 250 is rated at mechanical shaft power of 85kW, and has a name plate capacity of 70kW when accounting for mechanical and electrical losses within the overall system. The turbine design is optimized for high robustness, low-weight and a minimized complexity to achieve high reliability, low maintenance as well as simple and fast offshore installation with standard workboat. The turbine features a modular concept with one drivetrain for different sites and resources through an adjustable rotor diameter (D = 4 m, D = 4.3 m and D = 6.3 m versions have been built).

In the variant installed on PLAT-I 6.40 in Grand Passage, each turbine weighs 1.5 tons, has a diameter of D = 4 m. The drivetrain consists of a state-of-the-art hub-shaft connection including sealing package, a low speed shaft, a two-stage planetary gear-set with improved fatigue behaviour, squirrel cage asynchronous generator and a single dry mate connector providing the electrical interface. The reliability of the drivetrains was successfully tested in a test campaign by the *Centre for Wind Power Drives CWD* at the RWTH Aachen University [9].

The turbines have a fixed-pitch rotor with three passive adaptive blades made from fibre composites. Through a carefully designed and tested bent-twist coupling, the blades passively shed load in extreme conditions resulting in a lighter design of the load path components (see [10] and [11]). The hydrodynamic design has been optimized for high power-to-thrust ratios and minimal cavitation inception at a wide operating range blades as described in [4]. The predicted hydrodynamic performance has been validated prior in model-scale test campaigns. Specialized surface coatings provide high mechanical resistance and minimize biofouling.

The SIT 250 is operated at variable speed with the objectives of maximizing the power output and keep the operating point within limits of the system using a so called *overspeed* strategy. Until the turbine reaches the nominal mechanical shaft power of P_{rated} = 85 kW, the rotor speed is controlled such that the turbine operates at its optimal point. To limit the power of the turbine, the speed control is used to reduce the generator torque by increasing the rotor speed and thus allow controlled overspeed at water velocities above the nominal speed. Furthermore, the overspeed strategy allows the limitation of the torque to the restricting maximum given by the drivetrain for larger rotor diameters.

D. Power Control and Auxiliaries

The Power, Control and Instrumentation (PCI) system, housed in main compartment of the centre hull, controls the turbines and auxiliaries such as the cooling system, hydraulic power unit and bilge system. All sensor signals

are collected by the PCI to support the platform operation and control. 240 of the signals are sent to a shore based Supervisory Control and Data Acquisition (SCADA) system to enable detailed analysis of the platforms status and performance as well as the control of a platform array once more than one platform is deployed to a site. A Human Machine Interface (HMI), which can be accessed from the platform or remotely, provides control of the platform to the operator. The PCI prepares the power generated by the turbines to be fed into the main grid and provides protection of the electrical equipment against internal and external overloading. To minimize power losses on the way to shore, an onboard transformer steps up the voltage from the 440 V of the SITs and PCI to the 6.6 kV transmitting level. To ensure a reliable data transfer and remote access, the PCI houses a redundant communication system featuring an optical fibre and a WIFI link.

E. Environmental Monitoring System

Even though there was no indication of harm to the marine life during the operation of predecessor platform (PLAT-I 4.63) from 2018 to 2020 in Grand Passage (see e.g. [2]), the monitoring activities were intensified to observe the marine environment in the vicinity of the PLAT-I 6.40 device. The monitoring equipment includes video cameras, a hydrophone, an acoustic fish tag receiver, and the software to log in, store and process the data on board. The collected data is analysed by independent third-party reviewers to test the hypothesis that marine life is not coming into physical contact with the device. To this date, no negative impact was observed.

F. Offshore Balance of Plant

A mooring turret allows the passive alignment with the flow, thus eliminating the need for an orientation control at the turbines. The turret is connected to a geostationary mooring spread. The seabed conditions at Grand Passage is gravel/sand or glacial till. Hence, the drag embedment anchors selected for the deployment were Vryhof Stevshark Rex anchors. These are 5.5t anchors with 2.5t ballast in the fluke. The single fore/aft catenary moorings are comprised of hawsers connected to the mooring turret, lighter chain sections in the suspended water column, heavier chain sections along the bed to provide catenary restoring force. On top of the mooring turret, a slipring is mounted to allow transmission of electrical power and optical signals between the geostationary turret system and the rotating platform. This includes 6.6kV electrical power from/to the subsea cable, power supply of load shackles at the mooring line connections and the optical fibre for communication. A 1.3 km long subsea cable then connects the platform with the land-based substation.

G. Onshore Balance of Plant

The onshore substation represents the interface to the main grid and is the base for the communication with the platform. It is located close to the ferry port in Freeport, Nova Scotia, Canada. The subsea cable terminates here, and a transformer provides the required voltage step up from 6.6 kV of the MV system to the 12.47 kV of the main grid. A climatized 10' container houses the SCADA cabinet and communication equipment. Besides this container, the shore station is a pole mounted infrastructure as it's the industry standard in North America.

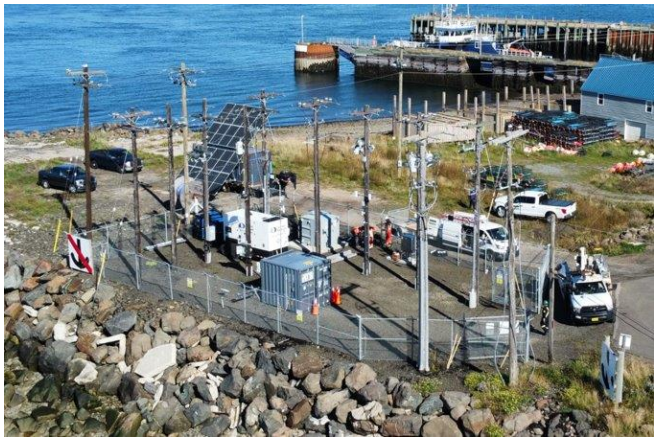

Fig. 5: Land-based substation with pole infrastructure, transformer and control container housing switch gear, communication basis and SCADA system.

The principal particulars of the PLAT-I 6.40 tidal energy platform are summarized in Table I

TABLE I:
PLAT-I 6.40 PLATFORM PRINCIPAL PARTICULARS

Platform Section	Parameter	Unit	Value
General	Installed Rated Power	kW	420
	Length Overall	m	33.5
	Breadth Overall	m	26.67
	Design Displacement	MT	140
	Lightship	MT	117
	Draught SDMs Down	m	Min 5.0
Centre Pontoon	Length Overall	m	33.5
	Breadth Overall (Exc. Sponsons)	m	2.4
	Breadth Overall (Inc. Sponsons)	m	3.6
	Depth	m	2.4
Side Pontoon	Length Overall	m	12.0
	Breadth Overall	m	2.4
	Depth	m	2.4
SIT250	No. of	-	6
	Rated power electrical	kW	70
	Rotor Diameter	m	4.0
	Hub Height	m	Min 3.0
	Blade Tip Immersion	m	Min 1.0
	Blade Tip Submergence	m	Min 5.0
	Tip to Tip Separation	m	Min 1

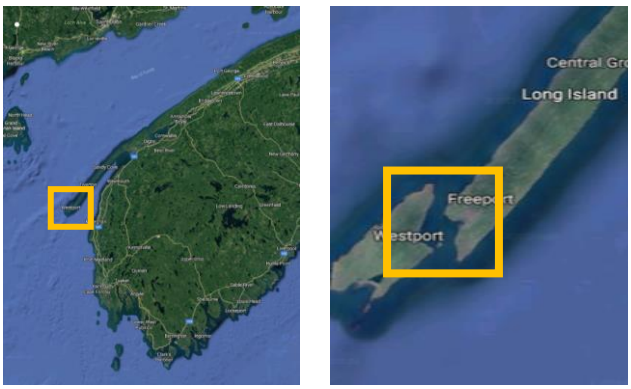

Fig. 6: Site Location in the Grand Passage, Nova Scotia, Canada (source: Google Maps)

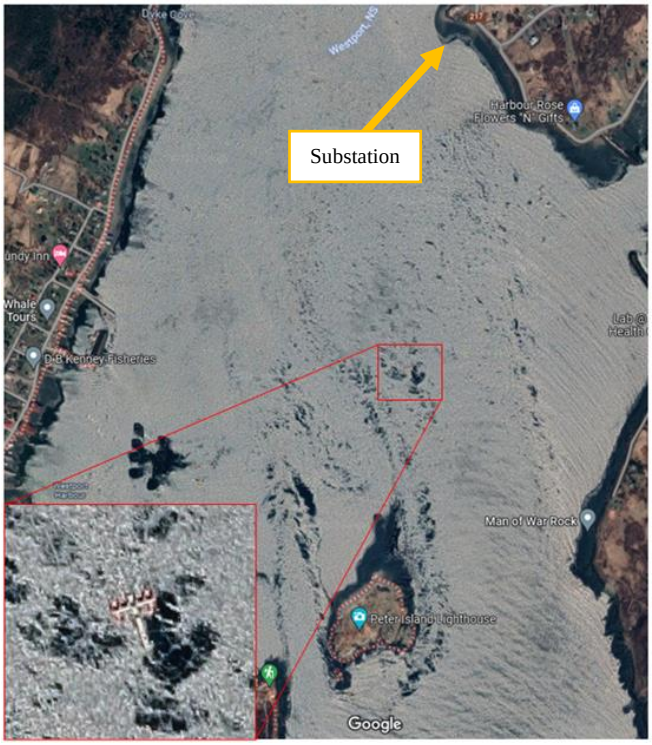

Fig. 7: PLAT-I 6.40 deployed in the Grand Passage, Nova Scotia, Canada (source: Google Maps)

III. Commissioning and Field Demonstration

Following the lunch of PLAT-I 6.40 in February 2021, the platform was deployed to the company's test site in the Grand Passage, Nova Scotia, Canada, shown in Fig. 6 and Fig. 7. It's a sheltered site with moderate flow speeds, nearby harbours and further infrastructure, making it an ideal site for offshore commissioning and testing of the PLAT-I system. The water depth at the chosen location in the passage is between 13 m and 21 m with maximal tidal ranges over 6 m. Fig. 8 shows the neap and spring tide chart for Grand passage. The site has flow speeds between 2 m/s and 2.7 m/s and 1.2 m/s and 2 m/s on the ebb, depending on the neap and spring cycle, typically represented by the tidal coefficient between 20 and 120. These variances in flow speed are caused by local forcing and bathymetry, e.g., channel narrowing upstream on flood and changes to depth on the ebb causing expansion and deceleration [2]. As shown in [2] the different flow conditions affect the performance of a tidal energy device. Consequentially, and in accordance with the IEC-TS-62600-200, performance assessment is conducted separately for and ebb and flood conditions. The flow direction during flood varies between 335° and 350° and 155° and 170° for the ebb.

PLAT-I 6.40 has been connected to the Canadian grid in May 2022. Between May and end of September 2022 the system has undergone comprehensive commissioning and performance trials. Even though the operating license is limited to daylight hours, the platform was operating well over 1000 h during that time span. The achieved availability was 83% with 70% of the operating days reaching at least 96%. Over 35,000 kWh were fed into the Canadian grid.

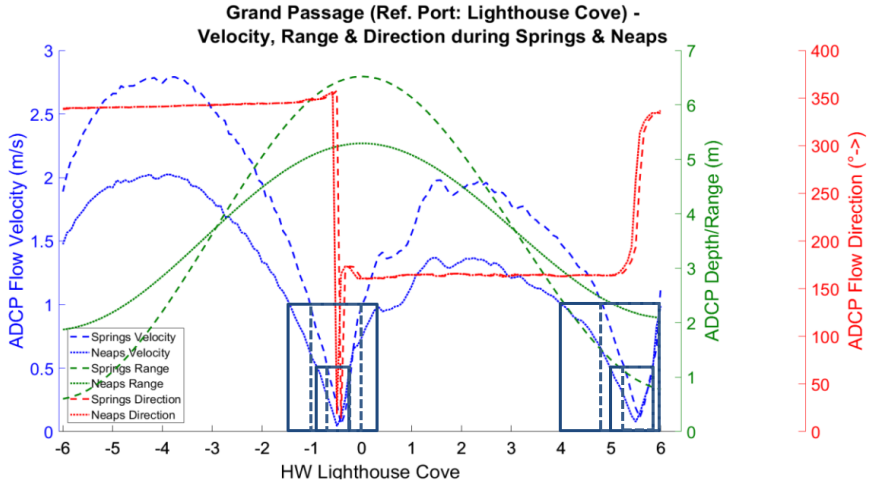

Fig. 8: Spring and neap tide chart for Grand Passage from [2]

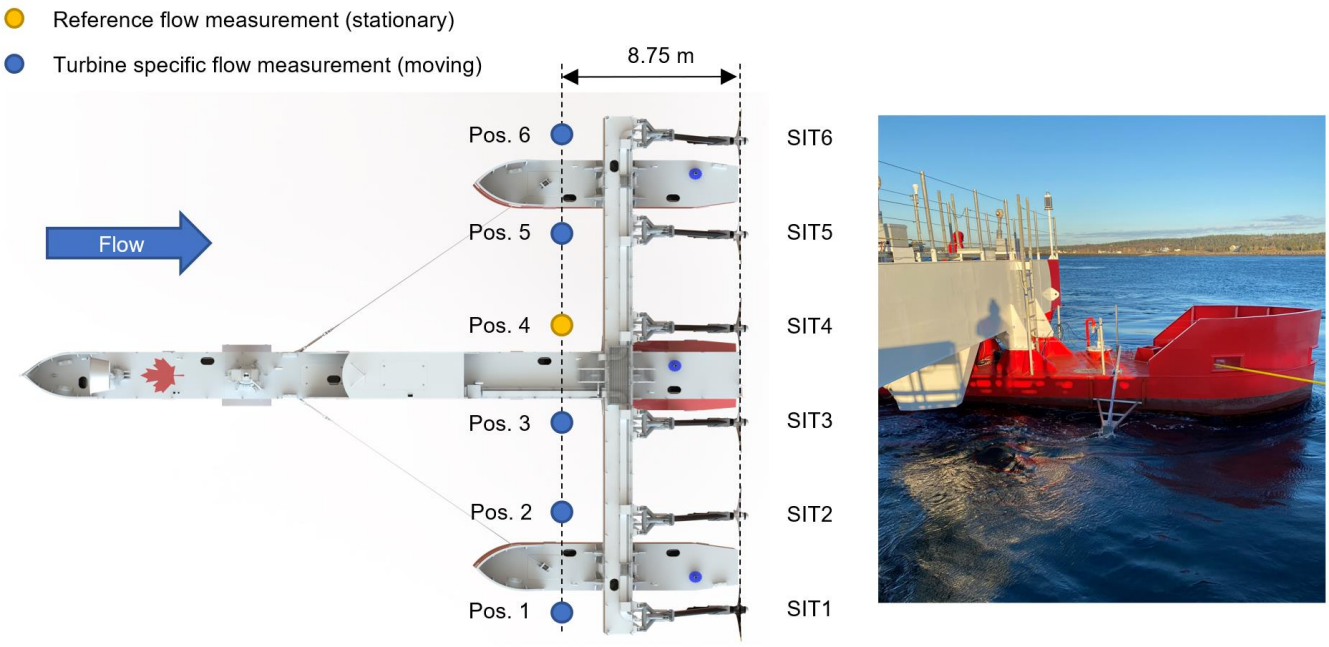

Fig. 9: Measurement setup on PLAT-I 6.40 - left: schematic of the velocity sensor positions; right: picture of the ECM mounted upstream of SIT2 using an aluminium A-frame rack.

IV. Test Methodology

A. Test Setup

To investigate if there are differences in the flow fields approaching the individual turbines, two flow speed sensors were used, the electro current meter (ECM) 803 from Valeport and an Acoustic Doppler Current Profiler (ADCP) from Teledyne RDI. The ADCP device was kept stationary over the full test period as reference while the ECM was subsequently positioned upstream of each turbine. The distance to the rotor plains was kept constant at 8.75 m for all measurements. The measurement setup is shown in Fig. 9. The positioning of the velocity sensors was predefined and restricted to the location of mounting aids for aluminium racks at the side of the pontoons that were used to deploy the sensors, exemplarily shown in the picture on the right side of Fig. 9. To have a single reference position, it was decided to place the ADCP as reference in front of SIT4. Consequently, the performance of SIT4 was used as reference as well. A fundamental difference between the velocity sensors is that the ECM measures the velocity at a single point while the ADCP able to take measurements throughout the water column, here every 0.5 m starting at 1 m below the water surface. The ECM takes measurements at ~0.5 m below the water surface.

All sensor signals sampled at a frequency of 1 Hz. The recorded data was not filtered. Table II summarizes the systems used for the performance assessment discussed in this paper.

TABLE II:
INSTRUMENTS AND SENSORS ON PLAT-I 6.40 USED FOR THE PERFORMANCE ASSESSMENT

Parameter	Instrument	Use
Velocity	ECM Model 803 Valeport	Flow speed ~2D upstream of the individual SIT250 turbines
Velocity	Teledyne RDI ADCP	Reference flow speed
Latitude/ Longitude	3x GPS at deckhouse, left and right side pontoon	Platform position, orientation, distinguish between flood and ebb conditions
Power	SIEMENS Simanics Inverter S120	Electrical power output of each SIT250 turbine at inverter input

B. Data Processing

The post-processing of the recorded data was done based on the IEC-TS-62600-200:2013 [8]. The applied procedure is briefly summarized in the following.

1) Calculate the instantaneous power weighted velocity $\widehat{U}_{i,j,n}$ across the swept area A of SIT4 as per equation 1, where k is the index number of the vertical current profiler bin, A_k is the portion of the rotor swept area at the *k-th* bin and $U_{i,j,k,n}$ is the magnitude of instantaneous velocity measured by the ADCP in the *k-th* bin.

$$\widehat{U}_{i,j,n} = \left[\frac{1}{A}\sum_{k=1}^{S} U_{i,j,k,n}{}^{3}\right]^{1/3} \quad (1)$$

2) Section the data in 2-minute time frames and calculate the mean power weighted current velocity $\overline{U}_{i,n}$ for each time frame, as per equation 2, where i is the flow velocity bin, j is the instantaneous velocity

data point, L is the number of instantaneous velocity data points, and n is the number of data points in a velocity bin. This step is done for the ADCP and the ECM, where for the latter case $\hat{U}_{i,j,n}$ is the measured magnitude of instantaneous velocity.

$$\bar{U}_{i,n} = \left[\frac{1}{L}\sum_{j=1}^{L} \hat{U}_{i,j,n}{}^{3}\right]^{1/3} \quad (2)$$

3) Calculate corresponding mean values of the respective data sources (power, platform orientation) for the 2-minute time frames.
4) Sort the time averaged data into the corresponding tide condition (separate ebb and flood data)
5) Sort the time averaged data according to the platform status. Within this work only data during the status *power production* is considered (turbines in operating position, inverters on, turbine power > 0 kW)
6) Sort the data into the corresponding flow velocity bins. For the work discussed in this paper, the ADCP data was used for the bin-sorting for comparisons and the ECM data when the performance of individual turbines was done.
7) Calculate mean value for each flow velocity and corresponding parameter in the *i-th* bin.

Mean bin equations for velocity $\bar{U}_i$ and electrical power at the frequency inverter $\bar{P}_{el,i}$ below. The bin increment was set to 0.1m/s.

$$\bar{U}_i = \frac{1}{N_i}\sum_{n=1}^{N_i} \bar{U}_{i,n} \quad (3)$$

$$\bar{P}_{el,i} = \frac{1}{N_i}\sum_{n=1}^{N_i} \bar{P}_{el,i,n} \quad (4)$$

V. RESULTS

The upper diagram in Fig. 10 shows the instantaneous power weighted flow speed across the swept area of SIT4 measured with the ADCP at position 4 (from now on referred as *reference flow speed* U_{ADCP}) over the test period discussed in this paper. The graph shows the 1 Hz raw data as well as the 2-mintue power weighted average. Between the 13th of August and 14th of August, the ADCP didn't record any data and hence this period had to be excluded from the analysis even though the platform was operating. In the lower diagram of Fig. 10 the corresponding electrical power output of the platform is shown again as 1 Hz raw data and the 2-minute time average. Furthermore, the time periods in which the ECM was installed at a certain position are highlighted. As the operating license was limited to daylight only, there was no power produced during night-time explaining the lengthier periods of no output power. Maintenance work

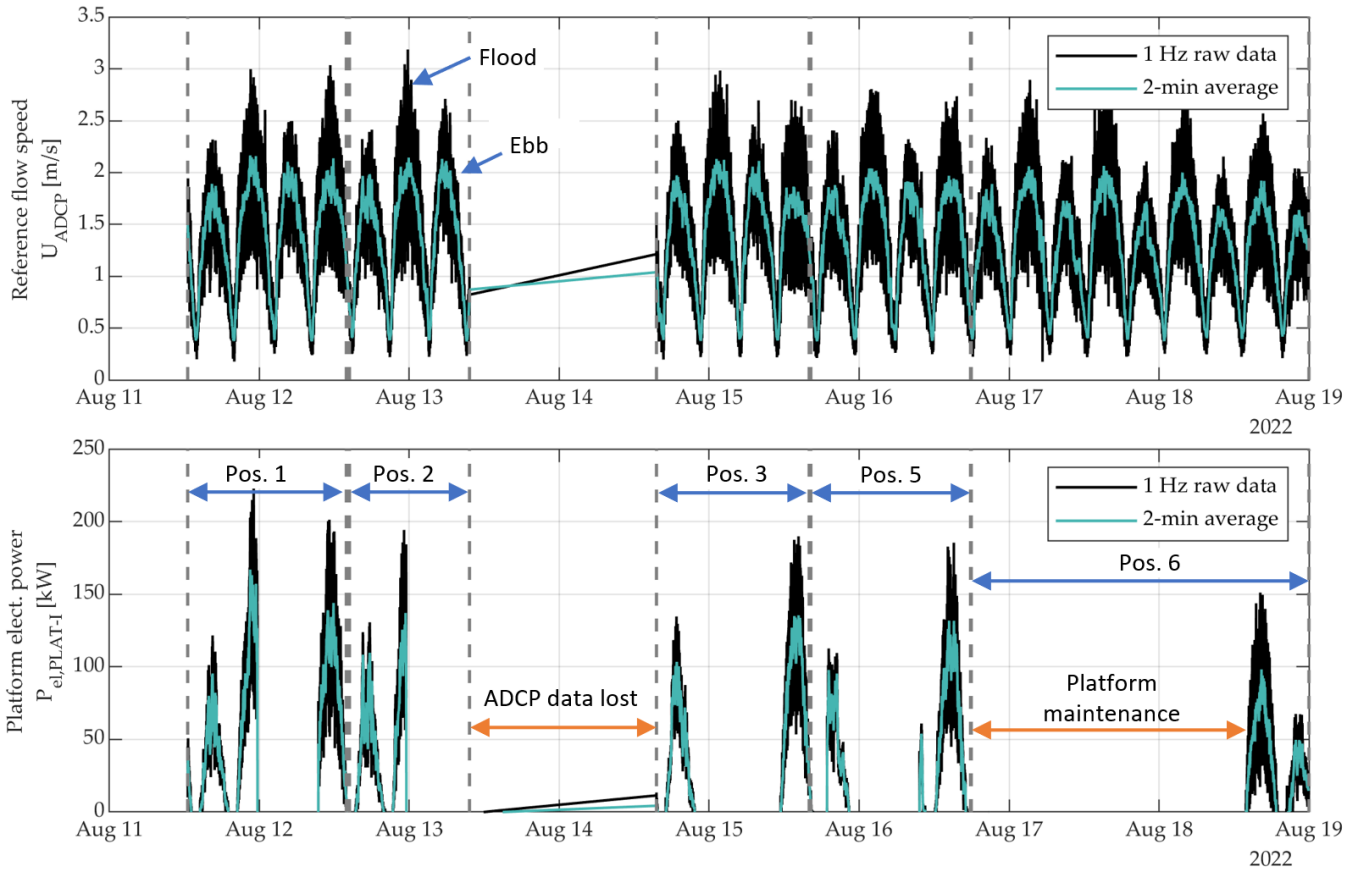

Fig. 10: Time series (1 Hz and 2-minute average) over the test period - upper: reference flow speed (i.e. power weighted velocity across the swept area of SIT4); lower: electrical power output of PLAT-I 6.40 before the onboard LV to MV transformer

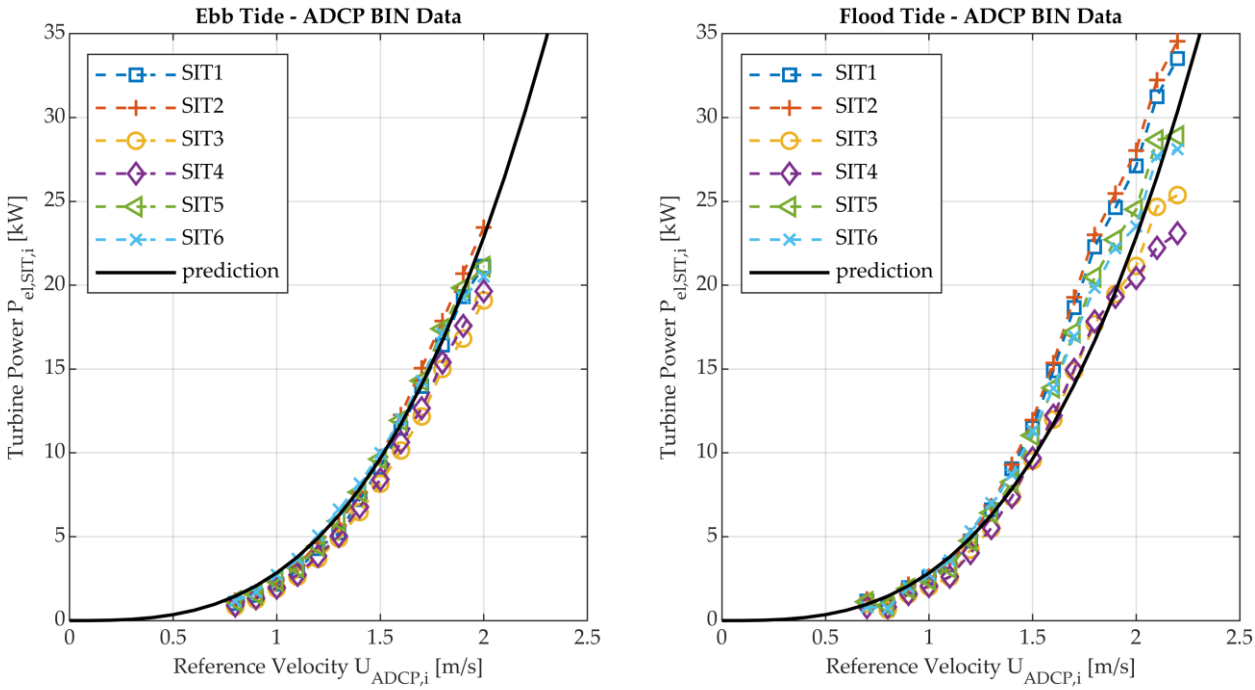

Fig. 11: Power curves of all six turbines based on the measurement data collected with the ADCP at position 4 over the test period and compared against the design predictions.

on the platform prohibited normal operation on the afternoon of the 16th of August and all of the 17th. As observed for the predecessor platform 4.63 and presented in [2], the flood tides are distinctively more powerful on this particular site, accompanied by an increase of turbulence leading to higher fluctuation of the power output during flood tides as well. Eventually, this leads to a larger spread of the corresponding power curves of the individual turbines shown in Fig. 11 as well. The ECM was installed at each position at least for one ebb and flood cycle, respectively.

The power curves shown in Fig. 11 were derived on basis of the reference flow speed U_{ADCP} and have been sorted according into ebb and flood tide data. The field data is compared against design predictions done with an in-house BEMT software [12]. In general, the turbines performed well, with meeting or excel the predictions. For both, ebb and flood tide, the inner two turbines, SIT3 and SIT4, are outperformed by the remaining SITs. This is less pronounced during ebb tide. During flood, the port side turbines, in particular SIT1 and SIT2, are performing better than their starboard counterparts, which is not the case for the ebb data.

Fig. 12 shows power curves of the individual SITs considering the flow speed measurements taken upstream of the respective turbine. The larger spread of the data can be explained by the reduced measurement time. While the data shown in Fig. 11 is based on the whole test period, the power curves presented in Fig. 12 are based on significantly shorter test periods (compare Fig. 10). However, the measured power is in general in good agreement with the design prediction. In contrast to Fig. 11, SIT3 is exceeding the predicted power curve and SIT6 is underperforming at ebb as well as at flood tide. The former implies that the flow speed measured close to water surface at position 3 is lower as compared to the power weighted average across the rotor swept area. The latter indicates, that the flow speed measured near the surface at position 6 is higher than the average experienced by SIT6.

Fig. 13 shows the bin-averaged deviations of the flow speed measured by the ECM at positions 1 to 6 compared reference flow speed at position 4. The graph is shown for 5 different reference flow speeds from 1 m/s to 1.8 m/s. To provide display the velocity's rate of change across the platform width, the deviation is plotted as function of the ECM's distance from the symmetry axis of PLAT-I. There is a clear tendency that there is a deficit in the flow field approaching SIT3. Since the measurement was taken at ~0.5 m below the water surface and the drought of the platform is around 0.8 m it's likely that the ECM measurements at position 3 are impacted by the boundary layer establishing on the side of the centre hull while this effect is less pronounced at the significantly shorter side pontoons. Under consideration of the performance analyses presented in Fig. 11 showing a very similar power output from SIT3 and SIT4, it seems like there is a general offset between the ECM and the ADCP of 0.1 to 0.2 m/s as one would expect the flow measured at position 3 to be similar to the reference velocity. However, qualitatively the deviations match the expectations based on the turbine performance with a distinctive velocity deficit at position 3. Fig. 4 shows that the mooring turret, and in particular table-like section to connect where the mooring lines are attached, are directly upstream (~5D distance) of large parts of the swept areas

of SIT3 and SIT4. Hence, a not fully recovered wake of this structure could cause a flow speed deficit at the rotor plain and therefore cause a reduced power output. An anomaly are the velocities measured at position 6 providing the similar or higher values as position 1 while the energy yield of SIT1 is higher than the one of SIT6. Interestingly, there is no clear tendency recognizable that the flow deviations are a function of mean flow speed, hence the relative deviation decreases with increasing flow speeds. Until now, there is no reasonable explanation found, why the surface near flow speeds are higher at position 6 for ebb and for flood.

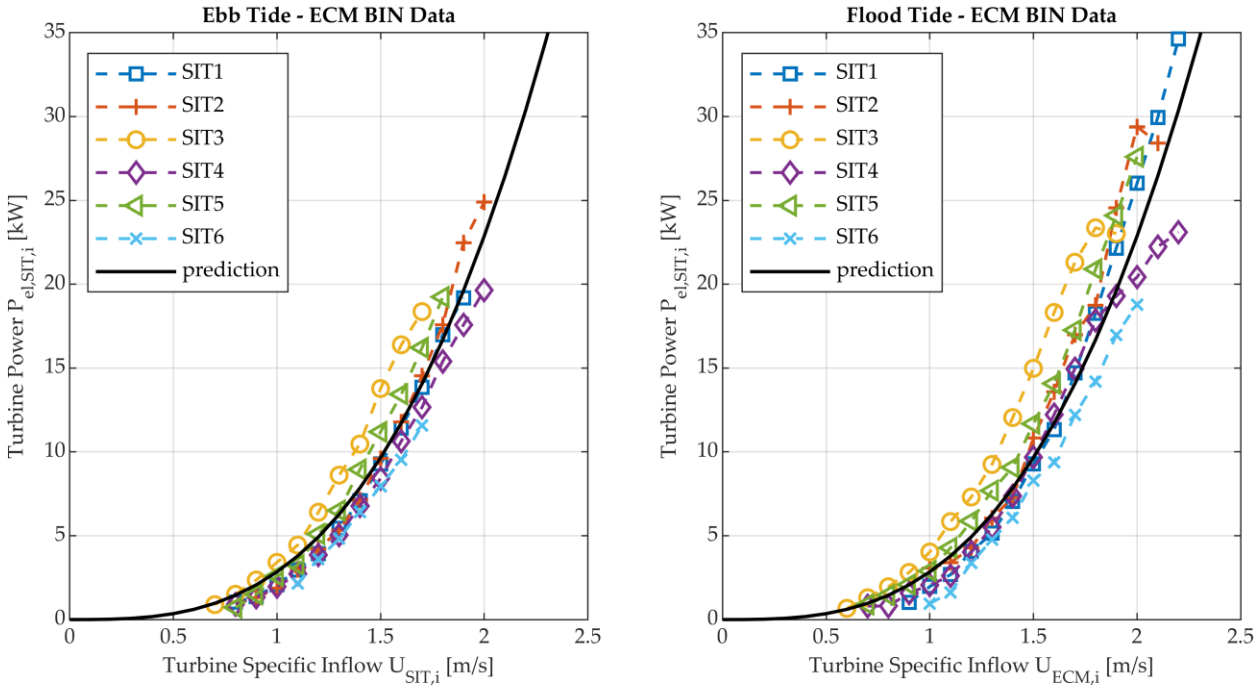

Fig. 12: Power curves of all six turbines based on the measurement data collected by the ECM upstream of the individual turbines and compared against the design predictions.

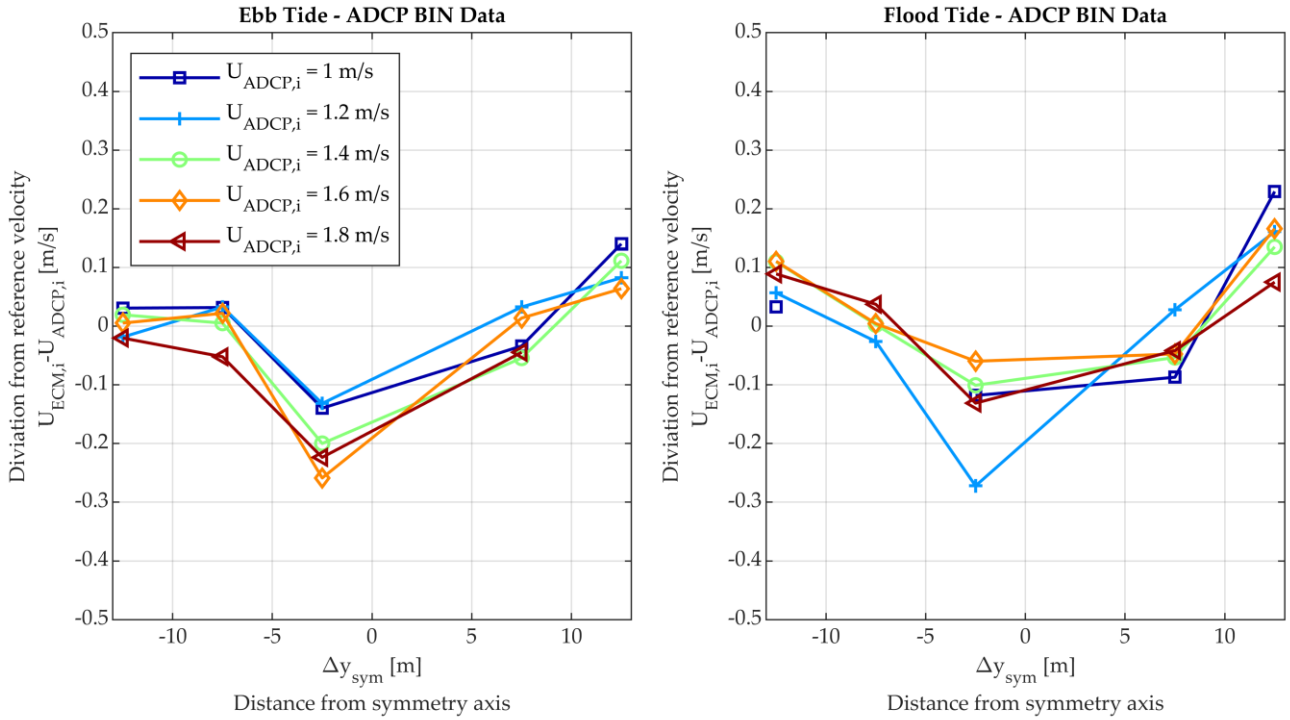

Fig. 13: Flow field across PLAT-I 6.40: deviation of the flow speed measured with the ECM at the positions 1 to 6 from the reference flow speed measured at position 4.

VI. Summary and Conclusion

This paper presented the results of a measurement campaign done on Sustainable Marine's multi-rotor floating tidal energy platform PLAT-I 6.40 in the Grand Passage, Nova Scotia, Canada, in August 2022. The tests were part of the commissioning and field demonstration of the newly designed and built system. The objective was to investigate differences in the power output across the platform's six turbines and the relation to variances in the approaching flow fields. Therefore, a single point ECM velocity sensor was subsequently positioned upstream of 5 out of the six turbines, while an ADCP was stationary upstream of one of the trimaran's inner turbines (starboard side). At each position flow speed and the turbine power was recorded over at least one flood and one ebb cycle. The turbines' power curves were derived guided by the IEC-ST-62600-200:2013 standard based on the flow speeds measured with the ADCP at the reference position as well as with the flow speeds measured with the ECM upstream of the individual turbines. Furthermore, the deviation of the ECM measurements to the reference flow speed was derived for each position.

In general, the turbines' performance is in good agreement with the design prediction. However, it was found that the inner two turbines are outperformed by the outer and middle ones when considering the reference flow speed. The power curves derived from the flow speeds measured directly upstream of the individual turbines indicate that this is due to a flow speed deficit in the middle of the trimaran-shaped platform. The comparison of the flow speeds measured at the individual positions across the platform and the reference values support this assumption. A possible explanation is that the wake of the mooring turret positioned ~5D upstream of the inner turbines causes the observed flow deficit and hence the reduced power output.

The results of the full-scale field tests presented in this work do not show a distinctive impact of rotor interaction effects on the performance of this multi-rotor system. However, it is possible that these effects are superposed by the impact of the mooring turret or reduced due to the high turbulence intensity.

Based on the findings presented in this work, hydrodynamic optimization of the shape of the mooring turret to minimize wake effects could further improve the performance the PLAT-I 6.40 multi-rotor system.

To improve the validity of the assumptions above, a reiteration of the test campaign is recommended with the following adaptions to the test setup:

- Positioning of the reference measurements upstream of the turret,
- Using only ADCP to take measurements across the rotors' swept areas and minimize the impact of surface effects and the platform on the measurements, and
- Increase the test period at for each position to improve reliability of the measured data.

Acknowledgement

This work has been supported by Natural Resources Canada within Energy Innovation Program.

References

[1] Ocean Energy Systems, "Tidal Current Energy Development Highlights 2023", May2023. [Online] Available: https://www.ocean-energy-systems.org/documents/10412-oes-2023-tidal-current-energy-spreads.pdf/

[2] Jeffcoate, J., et al." Comparisons between Flood and Ebb Performance of PLAT-I in Nova Scotia", Proceedings of the 14th European Wave and Tidal Energy Conference, September 2021, Plymouth, UK

[3] Van der Laan, M.P., et al., "Power curve and wake analyses of the Vestas multi-rotor demonstrator", Wind Energ. Sci., 4, 251–271, 2019, https://doi.org/10.5194/wes-4-251-2019

[4] Kaufmann, N., „Small Horizontal Axis Free-Flow Turbines for Tidal Currents" Shaker Verlag, Düren, 2019

[5] Jamieson, P., et al "Development of a multi rotor floating offshore system based on vertical axis wind turbines" J. Phys.: Conf. Ser. 2257 012002, 2022

[6] Stallard T., Collings R., Feng T. and Whelan J. 2013Interactions between tidal turbine wakes: experimental study of a group of three-bladed rotors" Phil. Trans. R. Soc. Vol. 371, 2013, https://doi.org/10.1098/rsta.2012.0159

[7] Joßberger, S., Stadler, C., Barkmann, U., Kaufmann, N., & Riedelbauch, S. (2022). Interaction between two horizontal axis tidal turbines in model scale – experiment and simulation. International Marine Energy Journal, 5(2), 173–182. https://doi.org/10.36688/imej.5.173-182

[8] Marine energy - Wave, tidal and other water current converters - Part 200: Electricity producing tidal energy converters - Power performance assessment, IEC TS 62600-200:2013.

[9] Rapp, T., Jacobs, G., Bosse, D. et al. Development of test methodologies for experimental lifetime investigations of tidal turbines. Forsch Ingenieurwes 85, 649–659 (2021). https://doi.org/10.1007/s10010-021-00456-z

[10] Kaufmann, N., Starzmann, R., Jaquemotte, P., "Full-Scale Static Testing of a Passive Adaptive Instream Turbine Blade", Proceedings of the 14th European Wave and Tidal Energy Conference, 2021, Plymouth, UK

[11] Glennon, C., Finnegan, W., Kaufmann, N. et al. Tidal stream to mainstream: mechanical testing of composite tidal stream blades to de-risk operational design life. J. Ocean Eng. Mar. Energy 8, 163–182 (2022). https://doi.org/10.1007/s40722-022-00223-4

[12] Kaufmann, N., Carolus, T., Starzmann, R., „An enhanced and validated performance and cavitation prediction model for horizontal axis tidal turbines" International Journal of Marine Energy, Vol. 19, 145-163, 2017